Progress in Natural Science: Materials International 26 (2016) 177–181

HOSTED BY

Contents lists available at ScienceDirect

Progress in Natural Science: Materials International

journal homepage: www.elsevier.com/locate/pnsmi

Original Research

Effect of Mg substitution for La on microstructure, hydrogen storage and electrochemical properties of $La_{1-x}Mg_xNi_{3.5}$ (x=0.20, 0.23, 0.25 at%) alloys

Wei Lv, Yufan Shi, Wanpeng Deng, Jianguang Yuan, Youhua Yan, Ying Wu *

Beijing Key Laboratory of Energy Nanomaterials, Advanced Technology & Materials Co., Ltd, China Iron & Steel Research Institute Group, No. 76 Xueyuannanlu, Haidian District, Beijing 100081, China

ARTICLE INFO

Article history:
Received 31 January 2016
Accepted 20 February 2016
Available online 20 April 2016

Keywords:
Hydrogen storage alloy
Mg substitution for La
Electrochemical property

ABSTRACT

The effect of Mg substitution for La on microstructure, hydrogen storage and electrochemical properties of the annealed $La_{1-x}Mg_xNi_{3.5}$ (x=0.20, 0.23, 0.25 at%) alloys have been studied. All the samples were mainly composed of $(LaMg)_2Ni_7$, $(LaMg)Ni_3$, and $LaNi_5$ phases. Mg substitution for La changed the phase abundance, but did not change the constitution of all phases, which is confirmed by the results of back-scattered SEM images and EDS analysis. The P–C isotherms indicated that the $La_{1-x}Mg_xNi_{3.5}$ alloys reversibly absorbed and desorbed hydrogen smoothly at 298 K. The hydrogen absorption cyclic stabilities of $La_{0.77}Mg_{0.23}Ni_{3.5}$ alloy after 5 hydrogen absorption/desorption cycles reached the maximum values of 91.9% and 96.0% at 298 K and 323 K, respectively. The hydrogen desorption capacity and plateau pressure for the $La_{0.77}Mg_{0.23}Ni_{3.5}$ alloy reached the maximum values of 1.055 *H/M* and 0.074 MPa, respectively. The desorption capacities of $La_{0.77}Mg_{0.23}Ni_{3.5}$ reached 0.193 *H/M* and 0.565 *H/M* in the first minute at 298 K and 323 K, respectively. Electrochemical property measurement indicated that $La_{1-x}Mg_xNi_{3.5}$ (x=0.20, 0.23, 0.25 at%) alloys possessed excellent activation capability and were completely activated within 3 cycles. Discharge capacities of $La_{1-x}Mg_xNi_{3.5}$ alloys reached 378.2 mA h/g (x=0.20 at%), 342.7 mA h/g (x=0.23 at%), and 369.6 mA h/g (x=0.25 at%), respectively. Moreover, energy density of $La_{0.77}Mg_{0.23}Ni_{3.5}$ alloy was much larger than that of $La_{0.80}Mg_{0.20}Ni_{3.5}$ alloy and nearly approaches the maximum value of $La_{0.75}Mg_{0.25}Ni_{3.5}$. Thus, the $La_{0.77}Mg_{0.23}Ni_{3.5}$ alloy exhibits optimum comprehensive properties of hydrogen storage and electrochemistry.

1. Introduction

The low cost La–Mg–Ni A_2B_7 type alloys with absolute advantages [1] of high hydrogen absorption/desorption efficiency, good electrochemical properties, and environmental friendliness have been considered as one of the most promising advanced materials [2], and would attract more and more global attention and occupy a large market sharing in the near future [3]. It is well known that elemental substitution is one of the most effective ways to modify the hydrogen storage and electrochemical properties of A_2B_7 type alloys [4], and in recent years, there has been many reports about the effect of Mg-addition on A_2B_7 type alloys [5–14].

Dong et al. [15] prepared $La_{0.75+x}Mg_{0.25-x}Ni_{3.5}$ (x=0, 0.05, and 0.1 at%) alloys by induction melting under high purity helium with 0.04 MPa in a water cooled copper crucible, and found that $La_{0.75}Mg_{0.25}Ni_{3.5}$ alloy exhibits higher discharge capacity (343.7 mA h/g) than the other two alloys, the cyclic stability of $La_{0.85}Mg_{0.15}Ni_{3.5}$ alloy is best in three alloys and its capacity retention rate is (67.36%) after 100 charging/discharging cycles. Zhang et al. [16] prepared $La_{0.8+x}Mg_{0.2-x}Ni_{3.5}$ (x=0−0.05 at%) alloys by vacuum induction furnace in a helium atmosphere under the pressure of 0.04 MPa, and annealing treatment at 1223 K for 8 h in vacuum, they found that the $La_{0.8}Mg_{0.2}Ni_{3.5}$ alloy has the highest discharge capacity of 366 mA h/g, while the $La_{0.85}Mg_{0.15}Ni_{3.5}$ alloy has the best cyclic stability of 86.9% after 100 charging/discharging cycles. Zhang et al. [17] synthesized $La_{2-x}Mg_xNi_7$ (x=0.3–0.6 at%) composites by induction melting in 0.4 MPa argon atmosphere, and annealing treatment in 0.2 MPa argon atmosphere firstly at 1223 K for 10 h and subsequently at 1123 K for 3 days, they found that the $La_{1.5}Mg_{0.5}Ni_7$ alloy exhibits good cyclic stability (S_{70}=85.8%) and highest discharge capacity (389.48 mA h/g), but the annealing time is too long for practical application. Monnier et al. [18] found that there is specific corrosion for $La_{1.5}Mg_{0.5}Ni_7$ due to the Mg addition, and he also suggested that a compromise requires should be established between the beneficial effect of Mg on the pressure plateau and capacity

* Corresponding author.
E-mail address: yingwu2000@hotmail.com (Y. Wu).
Peer review under responsibility of Chinese Materials Research Society.

http://dx.doi.org/10.1016/j.pnsc.2016.03.008

and its detrimental effect on the corrosion rate. By now, researches in electrochemical properties of A_2B_7 type alloys doped by Mg are still not sufficient and the range of doping amount of Mg is broad to a certain degree, hence more particular efforts on composition optimization are needed for the purpose of making a better practical application of A_2B_7 type alloys on nickel–metal hydride batteries. Meanwhile, few studies have paid attention to the effect of Mg on hydrogen storage properties of La–Mg–Ni A_2B_7 type alloys, so the application of this kind of alloys in gas-solid hydrogen storage areas is also necessary to be investigated.

In one word, more detailed work need to be carried out in order to develop the potential of La–Mg–Ni A_2B_7 type alloys in hydrogen storage and electrochemical properties. As the maximum solubility of Mg in $LaNi_{3.5}$ is low (up to a composition of $La_{0.75}Mg_{0.25}Ni_{3.5}$) [19], the annealed $La_{1-x}Mg_xNi_{3.5}$(x=0.20, 0.23, 0.25 at%) alloys are designed and prepared in this work. A systematic study about the effect of Mg content on microstructure, hydrogen storage, and electrochemical properties is studied in order to obtain the optimum proportion of the compositions for the alloys.

2. Experimental

2.1. Sample preparation

Ingots of $La_{1-x}Mg_xNi_{3.5}$ (x=0.20, 0.23, 0.25 at%) alloys were prepared by induction melting under helium atmosphere, the purity of all the component metals of La, Mg and Ni was at least 99.99 wt%. After melting, the samples were annealed at 1173 K in a vacuum furnace for 8 h, and then crushed and grinded into powders of −250 to +350 mesh.

2.2. Phase structure analysis

The phase structures of the samples were investigated by X-ray diffraction (XRD, D8 Discover), with Cu-Kα radiation operated at 40 mA and 40 kV. The XRD profiles were analyzed by software Jade 5.0 and FullProf. The microstructures and phase compositions were examined using a Nova Nanosem 450 scanning electron microscope (SEM) equipped with an energy dispersive X-ray spectrometer.

2.3. Pressure–composition isotherm (PCI) measurement

After 4 cycles of hydriding/dehydriding under a hydrogen pressure of 5 MPa at 573 K to make the samples completely activated, hydrogenation properties of the alloys were measured using an automatically controlled Sievert-type PCT-1SPWIN apparatus.

2.4. Electrode preparation and electrochemical measurement

Negative electrode pellets with 10 mm diameter were prepared by mixing alloy powder with Ni carbonyl powder in a weight ratio of 1:3 together, and pressing under a pressure of 10 MPa. The negative electrode pellets, positive electrode $Ni(OH)_2$/NiOOH, and reference electrode Hg/HgO were immersed in a 6 mol L^{-1} KOH electrolyte for 24 h in order to wet fully, and fixed on tri-electrode cell to measure electrochemical characteristics using a LANHE CT2001A apparatus with charged/discharged current density of 100 mA g^{-1}.

3. Results and discussion

3.1. Effect of Mg-substitution for La on microstructure of $La_{1-x}Mg_xNi_{3.5}$ alloys

The phase components and structure characteristics of the

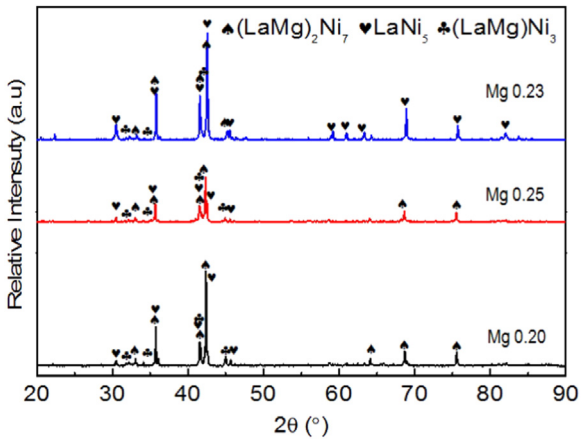

Fig. 1. XRD patterns of $La_{1-x}Mg_xNi_{3.5}$ alloys (x=0.20, 0.23, 0.25 at%).

$La_{1-x}Mg_xNi_{3.5}$ (x=0.20, 0.23, 0.25 at%) alloys are shown in Fig. 1. Evidently, all the alloys mainly contain three major phases of $(LaMg)_2Ni_7$, $LaNi_5$ as well as $(LaMg)Ni_3$. Based on the XRD data, the abundance and lattice parameters of the three major phases calculated by FullProf software are listed in Table 1. Increasing Mg content, phase abundance of $(LaMg)Ni_3$ and $LaNi_5$ firstly increases and then decreases, while the amount of $(LaMg)_2Ni_7$ phase firstly decreases and then increases. It is also seen that the increase of Mg content leads to the decrease of lattice parameters and cell volume to a certain degree.

Back-scattered SEM images of the $La_{1-x}Mg_xNi_{3.5}$ alloys are illustrated in Fig. 2, combining with EDS analysis, it's obvious that all the alloys mainly contain phases of $(LaMg)Ni_3$, $(LaMg)_2Ni_7$, as well as $LaNi_5$, which is consistent with the XRD analysis results.

Apparently, the variation of La/Mg ratio gives a clear change in the phase abundances instead of altering the phase composition, which is consistent with the relevant result of the previous report [17]. Mg substitution for La decreases the lattice parameters and cell volume at some degree, which should be attributed to the difference of atomic radius between Mg(1.72 Å) and La(2.74 Å) [15,20].

3.2. Effect of Mg-substitution for La on hydrogen absorption/desorption capacity of $La_{1-x}Mg_xNi_{3.5}$ alloys

Fig. 3 shows the pressure–composition isotherms (PCI) curves of the activated $La_{1-x}Mg_xNi_{3.5}$(x=0.20, 0.23, 0.25 at%) alloys reversibly absorbing and desorbing hydrogen at 298 K smoothly, and absorption/desorption plateau of $La_{0.77}Mg_{0.23}Ni_{3.5}$ alloy is higher, flatter and wider than that of the other two alloys. As shown in Table 2, the desorption capacities of the alloys are 1.055 *H/M* (x=0.23 at%), 1.021 *H/M* (x=0.2 at%), and 0.728 *H/M* (x=0.25 at%) respectively. Table 3 shows that the desorption capacity in the first minute is 0.193 *H/M* at 298 K and even reaches the maximum value of 0.565 *H/M* at 323 K.

As reported by Gao [21], $LaNi_3$ has higher hydrogen storage property than both La_2Ni_7 and $LaNi_5$, which probably means $(LaMg)Ni_3$ phase abundance plays a dominant role in the process of hydrogenation and dehydrogenation. So when Mg addition is 0.23, the hydrogen desorption capacity of $La_{1-x}Mg_xNi_{3.5}$ alloy with the highest $(LaMg)Ni_3$ phase abundance reach the maximum values, and its desorption capacity in the first minute is still outstanding.

3.3. Effect of Mg-substitution for La on hydrogen absorption/desorption cyclic stability of $La_{1-x}Mg_xNi_{3.5}$ alloys

The relationship of the hydrogen absorption/desorption capacities and cycle number of $La_{1-x}Mg_xNi_{3.5}$ alloys is shown in Fig. 4. The

Table 1
Summary of refinement data of $La_{1-x}Mg_xNi_{3.5}$ (x=0.20, 0.23, 0.25 at%) alloys.

Alloys	Major phase	Phase abundance/(wt%)	Lattice constant		
			a/Å	c/Å	Unit-cell volume/Å^3
$La_{0.8}Mg_{0.2}Ni_{3.5}$	$(LaMg)_2Ni_7$	73.29	5.08	24.338	542.86
	$(LaMg)Ni_3$	12.72	5.07	24.369	541.41
	$LaNi_5$	13.99	4.98	3.94	84.07
$La_{0.77}Mg_{0.23}Ni_{3.5}$	$(LaMg)_2Ni_7$	55.94	5.03	24.191	529.21
	$(LaMg)Ni_3$	21.91	5.02	24.246	529.99
	$LaNi_5$	22.15	4.97	3.92	83.71
$La_{0.75}Mg_{0.25}Ni_{3.5}$	$(LaMg)_2Ni_7$	88.13	5.06	24.281	537.97
	$(LaMg)Ni_3$	5.11	5.05	24.282	536.71
	$LaNi_5$	6.76	4.98	3.94	84.46

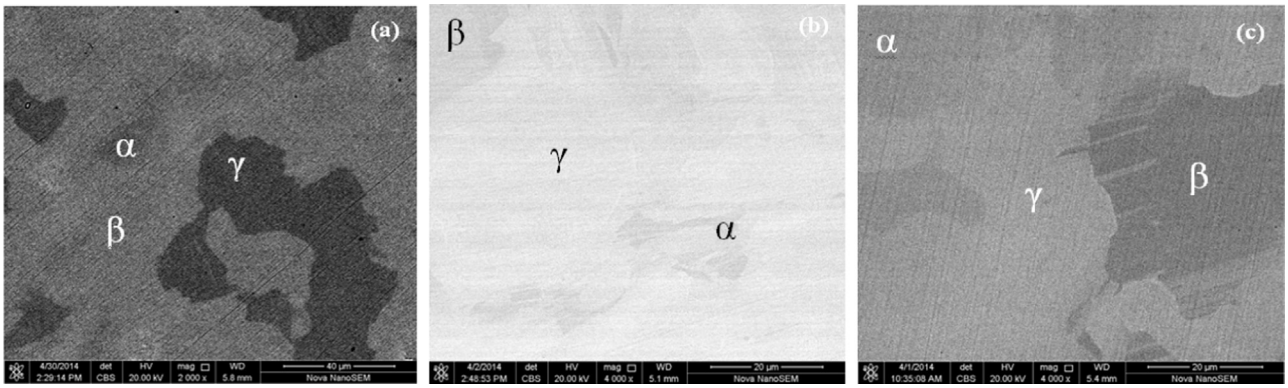

Fig. 2. Back-scattered SEM images of $La_{1-x}Mg_xNi_{3.5}$ alloys: (a) x=0.20, (b) x=0.23, (c) x=0.25. α:$(LaMg)Ni_3$, β:$(LaMg)_2Ni_7$, γ:$LaNi_5$.

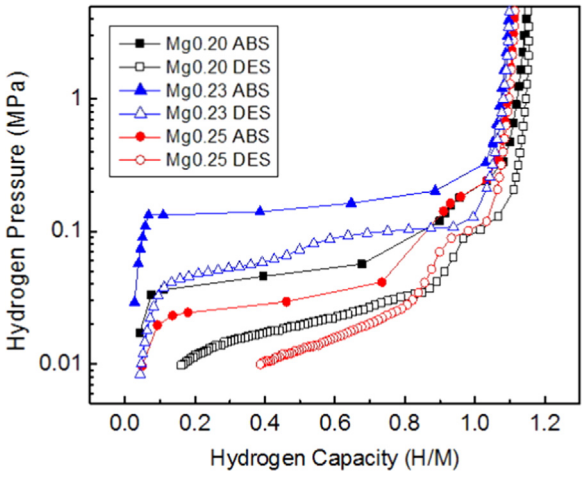

Fig. 3. P–C isotherms of $La_{1-x}Mg_xNi_{3.5}$ (x=0.20, 0.23, 0.25 at%) alloys at 298 K.

Table 2
Hydrogen absorption/desorption characteristics for $La_{1-x}Mg_xNi_{3.5}$(x=0.20, 0.23, 0.25 at%) alloys at 298 K.

Alloys	Hydrogen content (H/M) Desorption capacity	Plateau pressure (MPa) P_{DES}	Hysteresis factor
$La_{0.8}Mg_{0.2}Ni_{3.5}$	1.021	0.026	0.332
$La_{0.77}Mg_{0.23}Ni_{3.5}$	1.055	0.074	0.309
$La_{0.75}Mg_{0.25}Ni_{3.5}$	0.728	0.020	0.204

cyclic stability S_5 is calculated as $S_5=C_5/C_1\times 100\%$ (where C_1 and C_5 are the hydrogen absorption capacities at the first and the fifth cycle). Calculations demonstrate that S_5 at 298 K and 323 K reach the maximum values of 91.9% and 96.0% when Mg content is 0.23.

Table 3
Hydrogen absorption/desorption rate of $La_{1-x}Mg_xNi_{3.5}$(x=0.20, 0.23, 0.25 at%) alloys at 298 K and 323 K with an initial hydrogen pressure of 2 MPa.

Temperature (K)	Alloy	Desorption capacity in the first minute (H/M)
298	$La_{0.8}Mg_{0.2}Ni_{3.5}$	0.230
	$La_{0.77}Mg_{0.23}Ni_{3.5}$	0.193
	$La_{0.75}Mg_{0.25}Ni_{3.5}$	0.199
323	$La_{0.8}Mg_{0.2}Ni_{3.5}$	0.383
	$La_{0.77}Mg_{0.23}Ni_{3.5}$	0.565
	$La_{0.75}Mg_{0.25}Ni_{3.5}$	0.316

It is confirmed that the fundamental reason affecting cyclic stability of the alloy is the pulverization due to cell volume expansion in hydrogen absorption/desorption process [8,9]. The results from Fig. 5 indicate that the pulverization effect of $La_{0.77}Mg_{0.23}Ni_{3.5}$ alloy is minimal, and that is why S_5 reach the maximum values of 91.9% and 96.0% when Mg content is 0.23.

3.4. *Effect of Mg-substitution for La on electrochemical performances of $La_{1-x}Mg_xNi_{3.5}$ alloys*

As shown in Fig. 6, all the alloys possess excellent activation capability and can be completely activated within 3 cycles. As shown in Fig. 7, discharge capacities of $La_{1-x}Mg_xNi_{3.5}$ alloys reach 378.2 mA h/g (x=0.20 at%), 342.7 mA h/g(x=0.23 at%), and 369.6 mA h/g (x=0.25 at%) respectively, which are higher than 300 mA h/g of commercialized AB_5-type alloy electrodes [22]. As the key indicator for electrode materials' evaluation, energy density (W h/g) is defined as the battery energy storage per unit mass. Although the activation ability and discharge capacity of

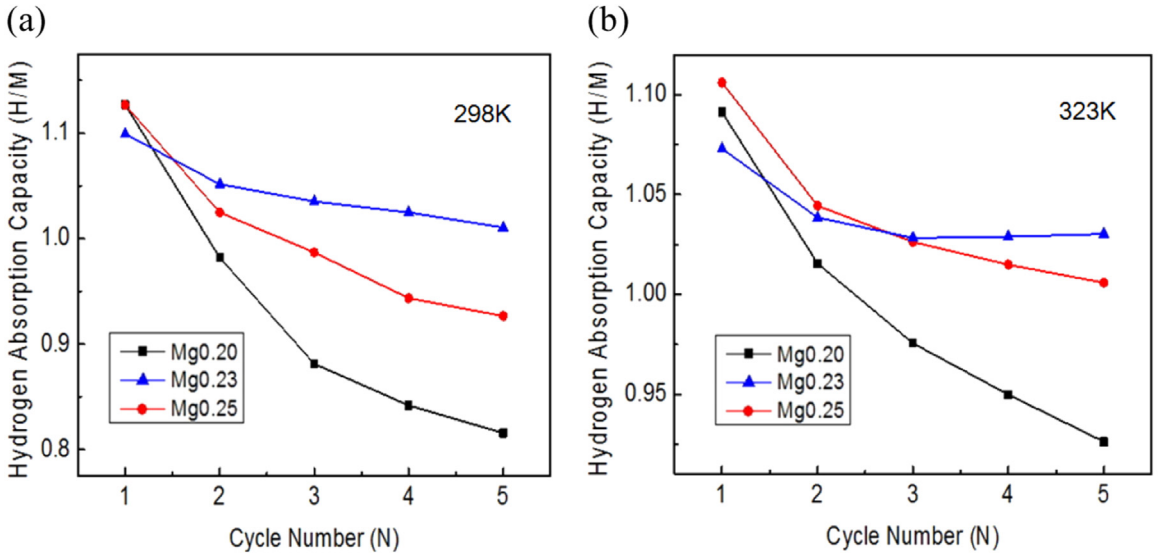

Fig. 4. Hydrogenation cyclic stability curves of $La_{1-x}Mg_xNi_{3.5}$ (x=0.20, 0.23, 0.25 at%) alloys at 298 K (a) and 323 K (b) with an initial hydrogen pressure of 2 MPa.

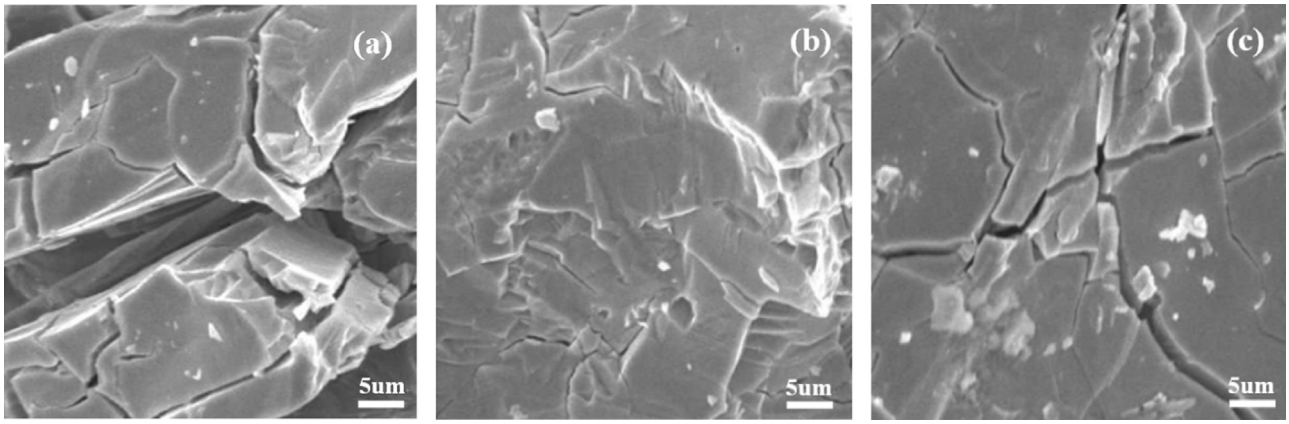

Fig. 5. SEM images of $La_{1-x}Mg_xNi_{3.5}$ alloys after 15 hydrogenation cycles at 298 K: (a) x=0.20, (b) x=0.23, (c) x=0.25.

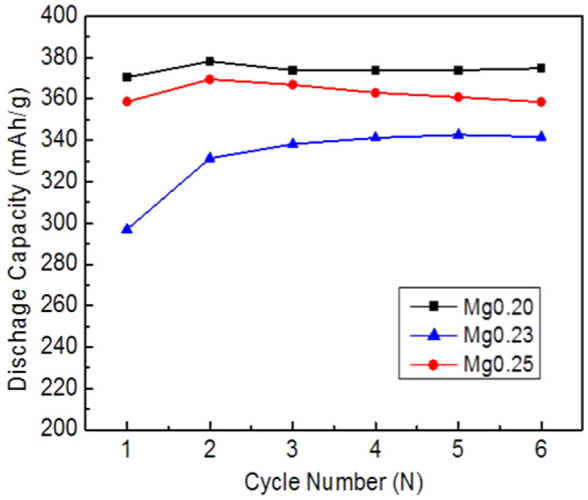

Fig. 6. Curves of the activation capabilities of $La_{1-x}Mg_xNi_{3.5}$ (x=0.20, 0.23, 0.25 at%) alloys.

$La_{0.77}Mg_{0.23}Ni_{3.5}$ alloy is not as good as that of the other two alloys, energy density of $La_{0.77}Mg_{0.23}Ni_{3.5}$ alloy is much larger than that of $La_{0.80}Mg_{0.20}Ni_{3.5}$ alloy and nearly approaches the maximum energy density value of $La_{0.75}Mg_{0.25}Ni_{3.5}$.

The reasons why $La_{0.77}Mg_{0.23}Ni_{3.5}$ alloy exhibits lower discharge capacity than that of the other two alloys might be ascribed as follows: firstly, some studies have shown that the activation ability and discharge capacity of $LaNi_3$ and $LaNi_5$ phases are lower than that of La_2Ni_7 phase [23–25], so the $La_{0.77}Mg_{0.23}Ni_{3.5}$ alloy with the maximum amount of $LaNi_5$ and $(LaMg)Ni_3$ phase exhibits lower activation ability and discharge capacity. Secondly, it was reported that the electrode with lower discharge potential has higher discharge capacity during charging process [26], and we can see clearly from Fig. 7 that the discharge potentials of $La_{1-x}Mg_xNi_{3.5}$ alloys are 0.726 V (x=0.20 at%), 0.808 V (x=0.23 at%), and 0.806 V (x=0.25 at%), respectively, so $La_{0.77}Mg_{0.23}Ni_{3.5}$ alloy with the highest discharge potential value exhibits lower discharge capacity. Thirdly, the discharge reduction of $La_{0.77}Mg_{0.23}Ni_{3.5}$ alloy also might be as a result of the decrease of available interstitial hole for hydrogen due to its small cell volume [27,28].

Furthermore, excellent energy density of $La_{0.77}Mg_{0.23}Ni_{3.5}$ alloy might be as a result of its minimal pulverization effect and phase boundaries among $(LaMg)_2Ni_7$, $LaNi_5$ as well as $(LaMg)Ni_3$ phases, which provides good tunnels for hydrogen atoms diffusion during charging and discharging process[29].

4. Conclusions

$La_{1-x}Mg_xNi_{3.5}$ (x=0.20, 0.23, 0.25 at%) alloys have been prepared by induction melting and annealing treatment, the effect of

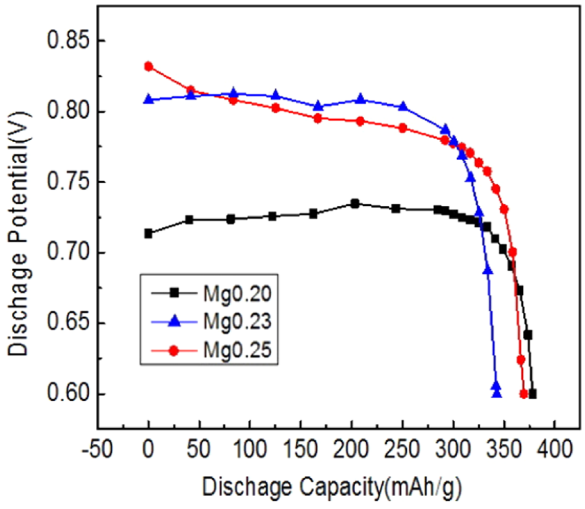

Fig. 7. Curves of discharge capacity and potential of $La_{1-x}Mg_xNi_{3.5}$ (x=0.20, 0.23, 0.25 at%) alloys.

Mg substitution for La on the microstructures, hydrogenation and electrochemical properties of the alloys has been investigated. The results obtained from the paper are summarized as follows:

(1) All the $La_{1-x}Mg_xNi_{3.5}$ alloys mainly contain three major phases of $(LaMg)_2Ni_7$, $LaNi_5$ as well as $(LaMg)Ni_3$. Increasing Mg content, phase abundance of $(LaMg)Ni_3$ and $LaNi_5$ firstly increases and then decreases, the amount of $(LaMg)_2Ni_7$ phase firstly decreases and then increases. Meanwhile, Mg substitution for La decreases the lattice parameter and cell volume at some degree.

(2) The $La_{1-x}Mg_xNi_{3.5}$ (x=0.20, 0.23, 0.25 at%) alloys reversibly absorb and desorb hydrogen at 298 K smoothly. The hydrogen desorption capacity and plateau pressure of $La_{0.77}Mg_{0.23}Ni_{3.5}$ alloy reach the maximum values of 1.055 *H/M* and 0.074 MPa, respectively.

(3) When Mg content is 0.23, the desorption capacities at 298 K and 323 K in the first minute reach 0.193 *H/M* and 0.565 *H/M*, respectively, and the cyclic stabilities after 5 hydrogen absorbing/desorbing cycles at 298 K and 323 K reach the maximum values of 91.9% and 96.0%, respectively.

(4) All the $La_{1-x}Mg_xNi_{3.5}$ alloys(x=0.20, 0.23, 0.25 at%) possess excellent activation capability and can be completely activated within 3 cycles, and the energy density of $La_{0.77}Mg_{0.23}Ni_{3.5}$ alloy is much larger than that of $La_{0.80}Mg_{0.20}Ni_{3.5}$ alloy and nearly approaches the maximum value of $La_{0.75}Mg_{0.25}Ni_{3.5}$, which reflects the potential application of $La_{1-x}Mg_xNi_{3.5}$ alloys appropriately.

Acknowledgment

This work was supported by the National Natural Science Foundation of China (Grant no. 51371056).

References

[1] T. Kohno, H. Yoshida, F. Kawashima, T. Inaba, I. Sakai, M. Yamamoto, M. Kanda, J. Alloy. Compd. 311 (2) (2000) L5–L7.
[2] B.G. Wang, L.F. Cheng, Z.L. Li, T.S. Huang, C.Z. Yang, J. Chin. Rare Earth Soc. 26 (2) (2008) 195–199.
[3] M.N. Guzik, B.C. Hauback, K. Yvon, J. Solid State Chem. 186 (2012) 9–16.
[4] S. Ma, M.X. Gao, R. Li, H.G. Pan, Y.Q. Lei, J. Alloy. Compd. 457 (2008) 458–464.
[5] S.H. Zhang, Y.C. Luo, S.P. Zeng, K. Wang, L. Kang, Chin. J. Rare Met. 37 (4) (2013) 512–520.
[6] J.L. Zhang, S.M. Han, Y. Li, J.J. Liu, S.Q. Yang, L. Zhang, J.D. Wang, J. Alloy. Compd. 581 (2013) 693–698.
[7] X.F. Liu, R.F. Li, C.C. Pan, B. Yang, R.H. Yu, Mater. China 30 (9) (2011) 26–29.
[8] L. Zhang, S.M. Han, Y. Li, J.J. Liu, J.L. Zhang, J.D. Wang, S.Q. Yang, Int. J. Hydrog. Energy 38 (2013) 10431–10437.
[9] Z.J. Gao, Y.C. Luo, R.F. Li, Z. Lin, L. Kang, J. Power Sources 241 (2013) 509–516.
[10] K. Young, T. Ouchi, B. Huang, J. Power Sources 248 (2014) 147–153.
[11] K. Young, T. Ouchi, B. Huang, J. Power Sources 215 (2012) 152–159.
[12] J.J. Liu, S.M. Han, Y. Li, X. Zhao, S.Q. Yang, Y.M. Zhao, Int. J. Hydrog. Energy 40 (2015) 1116–1127.
[13] J.J. Liu, S.M. Han, Y. Li, J.L. Zhang, Y.M. Zhao, L.D. Che, Int. J. Hydrog. Energy 38 (2013) 14903–14911.
[14] J.J. Liu, Y. Li, D. Han, S.Q. Yang, X.C. Chen, L. Zhang, S.M. Han, J. Power Sources 300 (2015) 77–86.
[15] X.P. Dong, F.X. Lu, Y.H. Zhang, L.Y. Yang, X.L. Wang, Mater. Chem. Phys. 108 (2008) 251–256.
[16] Y.H. Zhang, T. Yang, T.T. Zhai, Z.M. Yuan, G.F. Zhang, S.H. Guo, Trans. Nonferr. Met. Soc. China 25 (2015) 1968–1977.
[17] F.L. Zhang, Y.C. Luo, D.H. Wang, R.X. Yan, L. Kang, J.H. Chen, J. Alloys Compd. 439 (2007) 181–188.
[18] J. Monnier, H. Chen, S. Joiret, J. Bourgon, M. Latroche, J. Power Sources 266 (2014) 162–169.
[19] T.Z. Si, G. Pang, Q.A. Zhang, D.M. Liu, N. Liu, Int. J. Hydrog. Energy 34 (2009) 4833–4837.
[20] X.Q. Shen, Y.G. Chen, M.D. Tao, C.L. Wu, G. Deng, Z.Z. Kang, Int. J. Hydrog. Energy 34 (2009) 2661–2669.
[21] Z.J. Gao, Lanzhou University of Technology, Lanzhou 2007, pp. 9–11.
[22] F.L. Zhang, Y.C. Luo, K. Sun, D.H. Wang, R.X. Yan, L. Kang, J.H. Chen, J. Alloy. Compd. 424 (2006) 218–224.
[23] B. Liao, Y.Q. Lei, G.L. Lu, L.X. Chen, H.G. Pan, Q.D. Wang, J. Alloy. Compd. 356/357 (2003) 746–749.
[24] Y.H. Zhang, H.P. Ren, Y. Cai, T. Yang, G.F. Zhang, D.L. Zhao, Trans. Nonferr. Met. Soc. China 24 (2) (2014) 406–414.
[25] Y.H. Zhang, Z.H. Hou, T. Yang, G.F. Zhang, X. Li, D.L. Zhao, J Central S University Technol. 20 (5) (2013) 1142–1150.
[26] Z.W. Ma, D. Zhu, C.L. Wu, C.L. Zhong, Q.N. Wang, W.H. Zhou, L.S. Luo, Y.C. Wu, Y. G. Chen, J. Alloy. Compd. 620 (2015) 149–155.
[27] Y.H. Zhang, Z.H. Hou, B.W. Li, H.P. Ren, Y. Cai, D.L. Zhao, Trans. Nonferr. Met. Soc. China 23 (2013) 1403–1412.
[28] R.V. Denys, A.B. Riabov, V.A. Yartys, M. Sato, R.G. Delaplane, J. Solid State Chem. 181 (2008) 812–821.
[29] Y.J. Chai, K. Sakaki, K. Asano, H. Enoki, E. Akiba, T. Kohno, Scr. Mater. 57 (2007) 545–548.